**Discover** Oncology

Research

# MiR-493-5p functions as a tumour suppressor in head and neck squamous cell carcinoma progression by targeting HIF-1α

**Liu Jiahui[1,2,3,4] · Tian Ruxian[1,2,3,4] · Chen Xi[1,2,3,4] · Song Qing[5] · Sun Caiyu[1,2,3,4] · Li Dongxian[1,2,3,4] · Fang Yuhui[1,2,3,4,6] · Lv Shijun[1,2,3,4] · Yumei Li[1,2,3,4] · Xicheng Song[1,2,3,4]**

Received: 25 October 2024 / Accepted: 12 May 2025
Published online: 24 May 2025


## Abstract

**Background** Head and neck squamous cell carcinoma (HNSCC) demonstrates insidious onset, high prevalence, and low 5-year overall survival rate. While downregulation of miR-493-5p is implicated in the development of various cancers, its role in HNSCC remains unclear. Here, we explored the association of miR-493-5p with HNSCC progression and elucidated the underlying mechanisms.

**Methods** The miR-493-5p expression in HNSCC tissues and cells was verified by quantitative reverse transcription polymerase chain reaction (qRT-PCR). Cell proliferation and migration were detected by Cell Counting Kit 8, colony formation, and wound-healing assay. Dual-luciferase reporter gene assay was used to verify that miR-493-5p targeted hypoxia-inducible factor (HIF)-1α. Cobalt chloride ($CoCl_2$) was used to induce HIF-1α expression to perform rescue assays. SCC VII cells were used to construct the mouse model. After 15 days, the tumour volume was compared. The expression of HIF-1α, glycolysis, and epithelial–mesenchymal transition (EMT) proteins were verified by western blotting.

**Results** MiR-493-5p expression was low and beneficial to prognosis in HNSCC tumours. MiR-493-5p constrained HNSCC cell proliferation and migration and inhibited HIF-1α expression by targeting its 3′ untranslated region directly. $CoCl_2$ addition reduced miR-493-5p-induced cell proliferation, which may be related to the increased expression of HIF-1α. MiR-493-5p decelerated tumour cell growth in mice and was associated with glycolysis and EMT in HNSCC cells.

**Conclusions** MiR-493-5p, which targets HIF-1α and inhibits glycolysis and EMT, may be a novel therapeutic target for HNSCC.

**Keywords** Head and neck squamous cell carcinoma · MiR-493-5p · HIF-1α · Proliferation · Migration

## 1 Introduction

Head and neck cancer is the sixth most common cancer worldwide, according to Global Cancer Statistics 2022 [1]. Head and neck squamous cell carcinoma (HNSCC), developing in the mucosal epithelium of the oral cavity, pharynx, and larynx, is the most common cancer in the head and neck, with ever-increasing prevalence [2]. Although it can

Jiahui Liu, Ruxian Tian and Xi Chen contributed equally to the work.

✉ Yumei Li, myheart1263@163.com; ✉ Xicheng Song, drxchsong@163.com | [1]Department of Otorhinolaryngology, Head and Neck Surgery, Yantai Yuhuangding Hospital, Qingdao University, Yantai 264000, China. [2]Shandong Provincial Key Laboratory of Neuroimmune Interaction and Regulation, Yantai, China. [3]Shandong Provincial Clinical Research Center for Otorhinolaryngologic Diseases, Yantai, China. [4]Yantai Key Laboratory of Otorhinolaryngologic Diseases, Yantai, China. [5]Department of Otorhinolaryngology, Head and Neck Surgery, Yantai Yeda Hospital, Yantai, China. [6]The Second Medical College, Binzhou Medical University, Yantai, China.

be treated through surgery, radical radiotherapy, and other treatments, the 5-year survival rate of HNSCC is at 50% of cases due to late diagnosis and early lymph node metastasis [3]. However, the molecular mechanisms underlying HNSCC occurrence and development have not been fully elucidated. Therefore, identifying key molecules involved in HNSCC is highly warranted for the prediction of malignant progression, prognosis of patients, newer therapeutic targets, and therapeutic responses.

In humans, only about 2% of the ribonucleic acid (RNA) molecules produced through transcription are protein-coding messenger RNAs (mRNAs), whereas the remaining 98% are called noncoding RNAs (ncRNAs) [4]. MicroRNA (miRNA), a class of endogenous ncRNA with a length of approximately 22 nucleotides, can bind to the 3′ untranslated region (UTR) of its target mRNA to regulate the biological activity of cells [5]. Abnormal miRNA expression was noted to be correlated with cancer occurrence, progression, and patient prognosis for the first time in 2002 [6]. MiR-493-5p

**Table 1** Primer sequences in qRT-PCR

| Target gene | Primer (5′–3′) |
|---|---|
| miR-493-5p | F: 5′-GCCGAGTTGTACATGGTAGG-3′<br>R: 5′-CTCAACTGGTGTCGTGGA-3′ |
| U6 | F: 5′- CTCGCTTCGGCAGCACA –3′<br>R: 5′- AACGCTTCACGAATTTGCGT-3′ |
| HIF-1α | F: 5′- TATGAGCCAGAAGAACTTTTAGGC –3′<br>R: 5′- CACCTCTTTTGGCAAGCATCCTG –3′ |
| GAPDH | F: 5′- TGACTTCAACAGCGACACCCA –3′<br>R: 5′- CACCCTGTTGCTGTAGCCAAA –3′ |

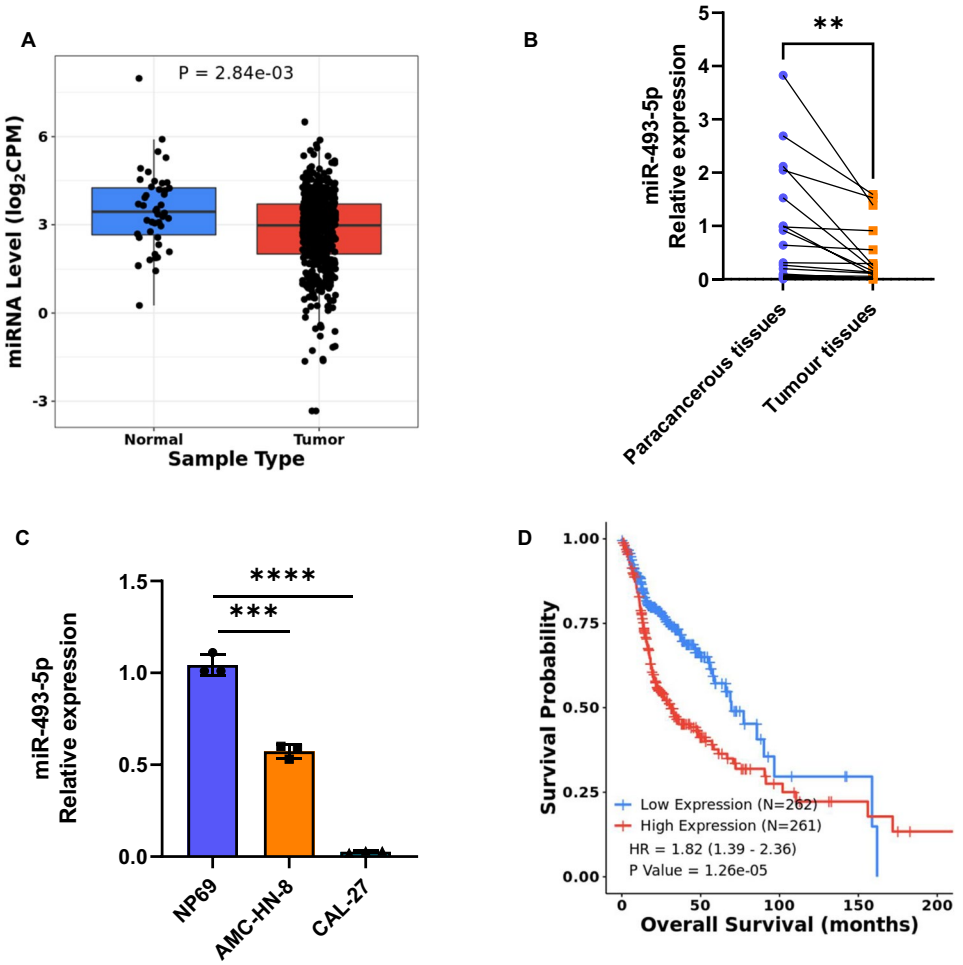


**Fig. 1** HNSCC tumours demonstrate low miR-493-5p expression. **A** Box plot of miR-493-5p expression data of normal (paracancerous tissue of HNSCC patients) and tumour tissues in the TCGA-HNSC data set. **B** MiR-493-5p levels in tumour and paracancerous tissue samples from patients with HNSCC analysed through qRT-PCR (n = 20). **C** MiR-493-5p levels in AMC-HN-8, CAL-27, and NP69 cells analysed through qRT-PCR. **D** Kaplan–Meier survival curves of HNSCC patients with low versus high miR-493-5p expression in the TCGA-HNSC data set. ** $p < 0.005$, *** $p < 0.0005$, **** $p < 0.0001$

can inhibit various cancers, including colorectal cancer [7], glioma [8], non–small-cell lung cancer [9], liver cancer [10], laryngeal cancer [11], breast cancer [12] and osteosarcoma [13]. The roles of miR-493-5p in HNSCC, however, remain unclear.

Hypoxia-inducible factor (HIF)−1α, a transcription factor crucial in a hypoxic environment, is essential for cancer cell development [14]. HIF-1α is strongly expressed in most cancers, such as breast [15], colorectal [16], ovarian [17] and oesophageal [18] cancers, where it promotes glycolysis [19–21] and epithelial–mesenchymal transition (EMT) [22] in cancer cells. Our gene target site prediction using TargetScan database (http://www.targetscan.org/) [23] indicated that HIF-1α may be a target of miR-493-5p; however, mechanisms through which miR-493-5p influence HNSCC progression by targeting HIF-1α remain unclear.

In the current study, we analysed the expression of miR-493-5p in tissue samples from patients with HNSCC and explored the effects of miR-493-5p on HNSCC in vivo and in vitro. We then investigated possible mechanisms by which miR-493-5p affects HNSCC by targeting HIF-1α. Our results may provide a new direction for HNSCC treatment research.

**Table 2** Clinical characteristics of HNSCC patients in the miR-493-5p low expression group and high expression group in TCGA dataset

| Characteristics | Low expression *n*(%) | High expression *n*(%) | *P* |
|---|---|---|---|
| Age (years) | | | 0.251 |
| ≤ 65 | 177 (67.6%) | 164 (62.8%) | |
| > 65 | 84 (32.1%) | 97 (37.2%) | |
| Unknown | 1 (0.4%) | 0 (0.0%) | |
| Gender | | | 0.357 |
| Female | 73 (27.9%) | 68 (26.1%) | |
| Male | 189 (72.1%) | 193 (73.9%) | |
| Clinical stage | | | 0.330 |
| I | 7 (2.7%) | 14 (5.4%) | |
| II | 43 (16.4%) | 54 (20.7%) | |
| III | 54 (20.6%) | 51 (19.5%) | |
| IV | 150 (57.3%) | 136 (52.1%) | |
| Unknown | 8 (3.1%) | 6 (2.3%) | |
| T stage | | | 0.813 |
| T1 | 18 (6.9%) | 19 (7.3%) | |
| T2 | 77 (29.4%) | 72 (27.6%) | |
| T3 | 71 (27.1%) | 67 (25.7%) | |
| T4 | 86 (32.8%) | 97 (37.2%) | |
| Tx | 7 (2.7%) | 5 (1.9%) | |
| Unknown | 3 (1.1%) | 1 (0.4%) | |
| N stage | | | 0.441 |
| N0 | 113 (43.1%) | 130 (49.8%) | |
| N1 | 40 (15.3%) | 44 (16.9%) | |
| N2 | 92 (35.1%) | 73 (28.0%) | |
| N3 | 4 (1.5%) | 5 (1.9%) | |
| Nx | 10 (3.8%) | 8 (3.1%) | |
| Unknown | 3 (1.1%) | 1 (0.4%) | |
| M stage | | | 0.409 |
| M0 | 244 (93.1%) | 248 (95.0%) | |
| M1 | 5 (1.9%) | 1 (0.4%) | |
| Mx | 10 (3.8%) | 10 (3.8%) | |
| Unknown | 3 (1.1%) | 2 (0.8%) | |

**Fig. 2** MiR-493-5p inhibits HNSCC cell proliferation and migration. **A**, **B** The expression of miR-493-5p in AMC-HN-8 and CAL-27 cells between the miR-493-5p-regulated and control groups detected by qRT-PCR. **C**, **D** Differences in AMC-HN-8 and CAL-27 cells' proliferation between the miR-493-5p-regulated and control groups measured using CCK-8 assay. **E**, **F** Differences in AMC-HN-8 and CAL-27 cells' colony-forming potential between the miR-493-5p-regulated and control groups measured using colony formation assays. **G**, **H** Differences in AMC-HN-8 and CAL-27 cells' migratory abilities between the miR-493-5p-regulated and control groups measured using wound-healing assay (magnification, 40 ×). *$p < 0.05$, **$p < 0.005$, ***$p < 0.0005$, ****$p < 0.0001$

## 2 Methods

### 2.1 Patient sample collection

We collected tumour tissues and matched paracancerous samples, mainly mucosa 5 mm away from the tumour tissues, from 20 patients undergoing surgical treatment for HNSCC at the Department of Otolaryngology, Head and Neck Surgery, Yantai Yuhuangding Hospital, Qingdao University. All samples were frozen immediately in liquid nitrogen after collection and then stored at − 80 °C for preparation. None of the included patients had received local or systemic treatment before sample collection. All patients provided written informed consent, and this study was approved by the Ethics Committee of Yantai Yuhuangding Hospital (no.: 2024-565)—all consistent with the Declaration of Helsinki. Clinical information for HNSCC patients from The Cancer Genome Atlas (TCGA) Head-Neck Squamous Cell Carcinoma Collection (HNSC) dataset was downloaded from the CancerMIRNome website (http://bioinfo.jialab-ucr.org/CancerMIRNome/).

### 2.2 Cell culture

The human laryngeal squamous cell carcinoma cell line AMC-HN-8 and the immortalized normal nasopharyngeal epithelial cell line NP69 were obtained from the Cell Bank of the Chinese Academy of Sciences (Shanghai, China), whereas the human tongue squamous cell carcinoma cell line CAL-27 and the mouse squamous cell carcinoma cell line SCC VII were procured from American Type Culture Collection (ATCC). All cells were grown in RPMI-1640 medium (Biological Industries, Kibbutz Beit Haemek, Israel) supplemented with 10% foetal bovine serum (Sbjbio, Nanjing, China) at 37 °C in a humidified 5% $CO_2$ incubator.

### 2.3 Cell transfection

MiR-493-5p mimic, inhibitor, and corresponding control constructs were purchased from GenePharma (Shanghai, China). AMC-HN-8 and CAL-27 cells were transfected using Lipofectamine 3000 (Thermo, Waltham, USA), according to the manufacturer's instructions. At 48 or 72 h after transfection, RNAs and proteins were isolated for quantitative reverse transcription polymerase chain reaction (qRT-PCR) and Western blotting.

LV-miR-493-5p (a miR-493-5p overexpression lentivirus) and its control (LV-NC mimic), constructed by GenePharma, were transfected into SCC VII cells, according to the manufacturer's instructions. At 72 h after transfection, the cells were selected using 2.5 μg/mL puromycin (Biosharp, Hefei, China). After the construction of a stable cell line, RNA was isolated for qRT-PCR.

### 2.4 Cobalt chloride treatment

The hypoxia-inducing drug cobalt chloride ($CoCl_2$) was purchased from Damao Chemical Reagent Factory (Tianjin, China). AMC-HN-8 and CAL-27 cells were plated in six-well plates and allowed to adhere. Next, the cells were treated with 50 μM $CoCl_2$ for 24 h directly or after 72 h of miR-493-5p mimic transfection. Finally, proteins were isolated from the cells for Western blotting.

### 2.5 qRT-PCR

We used the traditional methods for RNA isolation. In brief, total RNA was isolated from cells or tissues using SparkZol Reagent (Sparkjade, Shandong, China), and RNA concentration was measured on a spectrophotometer from Thermo. MiRNA and mRNA (1 μg) were inversely transcribed into complementary deoxyribonucleic acid (cDNA) using the miRNA

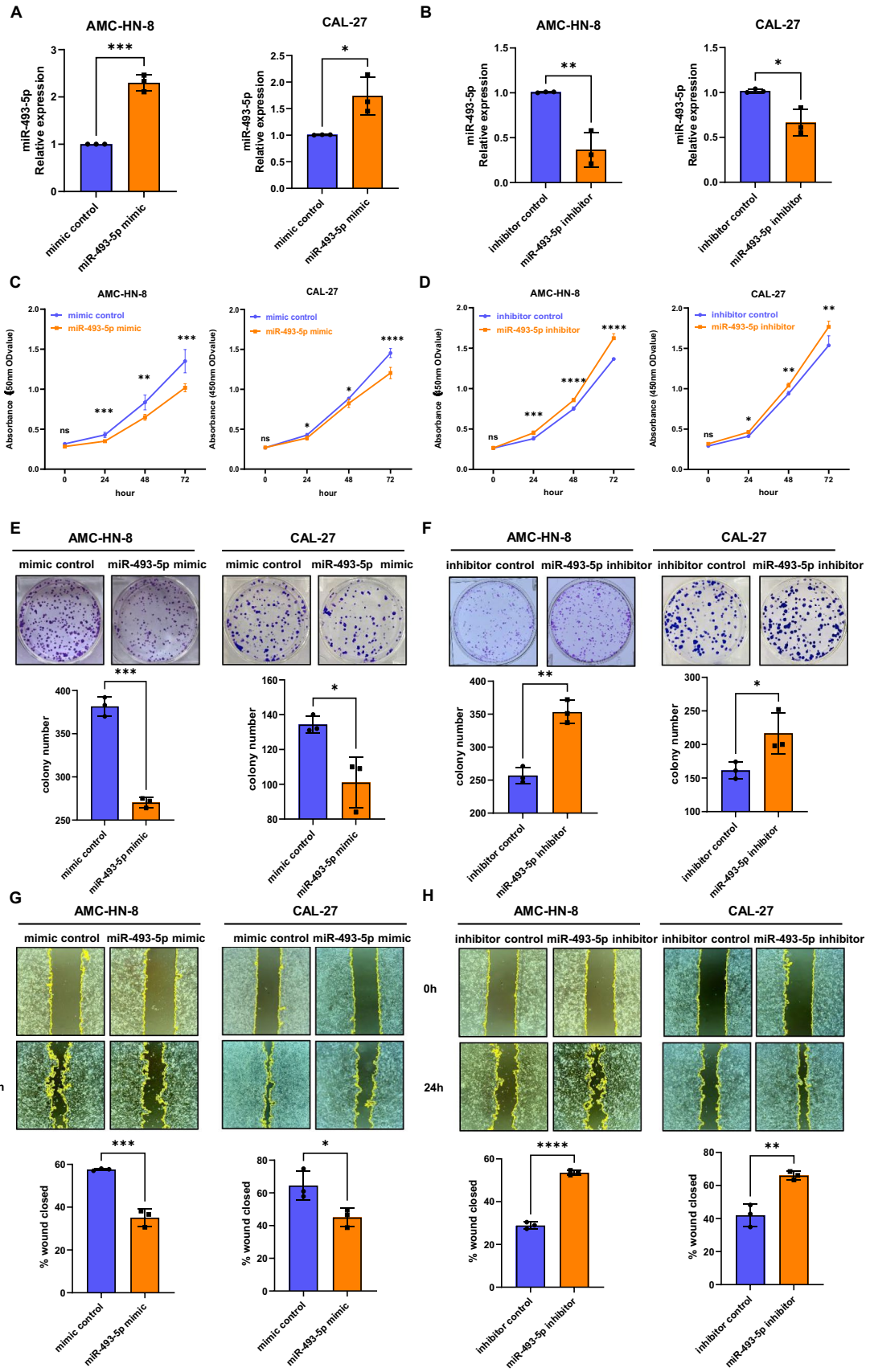
A
AMC-HN-8
CAL-27
miR-493-5p Relative expression
mimic control
miR-493-5p mimic
B
AMC-HN-8
CAL-27
inhibitor control
miR-493-5p inhibitor
C
AMC-HN-8
CAL-27
mimic control
miR-493-5p mimic
Absorbance (450nm ODvalue)
hour
D
AMC-HN-8
CAL-27
inhibitor control
miR-493-5p inhibitor
E
AMC-HN-8
CAL-27
colony number
F
AMC-HN-8
CAL-27
G
AMC-HN-8
CAL-27
0h
24h
% wound closed
H
AMC-HN-8
CAL-27

**Fig. 3** HIF-1α is a target of miR-493-5p. **A** Putative binding sites of miR-493-5p on HIF-1α 3′-UTR. **B**, **C** *HIF1 A* mRNA expression in AMC-HN-8 and CAL-27 cells from the miR-493-5p-regulated and control groups. **D**, **E** HIF-1α expression in AMC-HN-8 and CAL-27 cells from the miR-493-5p-regulated and control groups. **F** Dual-luciferase reporter gene assay verifying the binding relationship of miR-493-5p and HIF-1α. $^{*}p < 0.05$, $^{**}p < 0.005$, $^{***}p < 0.0005$

1 st strand cDNA synthesis kit (AG, Hunan, China) and HiScript II Q RT SuperMix for qPCR (+ gDNA wiper; Vazyme, Nanjing, China), respectively. We used the SYBR Green Premix Pro Taq HS qPCR Kit II (AG) to detect miR-493-5p expression with U6 as the normalization control [24], and used 2 × SYBR Green qPCR Mix (Sparkjade) to detect HIF-1α expression with GAPDH as the normalization control. All primers used here are listed in Table 1. All assays were conducted with the FTC-3000 real-time fluorescence quantitative PCR system (Funglyn, Shanghai, China), and the $2^{-\Delta\Delta Ct}$ method was used to assess relative gene expression. For each group, at least three independent replicates were used.

## 2.6 Western blotting

We used RIPA buffer (Sparkjade) and phenylmethylsulfonyl fluoride (PMSF; Sparkjade) to extract total protein from cells for 30 min. The proteins were quantified using a BCA protein assay kit (Sparkjade). They were then separated through 7.5% or 10% sodium dodecyl sulphate polyacrylamide gel electrophoresis (Epizyme, Shanghai, China) and transferred onto nitrocellulose filter membranes (Pall, Beijing, China). Antibodies against E-cadherin, N-cadherin, and glucose transporter type 1 (GLUT-1) were obtained from Proteintech (Wuhan, China), and antibodies against pyruvate dehydrogenase kinase 1 (PDHK1) and lactate dehydrogenase A (LDHA) were procured from Cell Signaling Technology (Danvers, USA). β-actin (Proteintech) was used as the internal reference. Tris(hydroxymethyl)aminomethane (Tris) buffer (Solarbio, Beijing, China) containing 0.1% Tween-20 (Sparkjade) and 5% nonfat milk (Coolaber, Beijing, China) was used to block the membrane at room temperature for 1 h. Subsequently, the membranes were cut prior to hybridisation with antibodies, and then incubated with primary antibodies against HIF-1α (Santa Cruz Biotechnology, Santa Cruz, USA) or any of the above at 4 °C overnight, respectively. Next, after rinsing with tris buffered saline with Tween-20 (TBS-T) three times (once every ten minutes), we incubated the membranes with horseradish peroxidase–labelled antirabbit (Affinity Biosciences, Cincinnati, USA) or antimouse (Abbkine, Wuhan, China) secondary goat immunoglobulin G H&L at room temperature for 1.5 h. Finally, the membranes were rinsed again, immersed in an ECL reaction solution (Yeasen, Shanghai, China) for colour development, and assessed on an enhanced chemiluminescence detection system (Tanon4800; Tanon, Shanghai, China).

## 2.7 Cell proliferation and colony formation assay

A Cell Counting Kit (CCK) 8 (Sparkjade) was used to assess cellular proliferation, according to the manufacturer's instructions. In brief, 24 h after transfected with miR-493-5p mimic or inhibitor, and corresponding control, cells were inoculated into 96-well plates at $3 \times 10^3$ cells per well with 100 µL of complete medium per well. After 24, 48, and 72 h, 10 µL of CCK-8 reagent was added to each well, followed by incubation at 37 °C for additional 2 h. Absorbance was then measured at 450 nm on a microplate reader (Thermo) to obtain the 450 nm Optical density (OD) value. For rescue assay, cells transfected with miR-493-5p mimic, miR-493-5p mimic and $CoCl_2$ treatment, and corresponding control were inoculated and cultured as above. After 24 h, the 450 nm OD value was obtained as above.

For colony formation assay, AMC-HN-8 and CAL-27 cells transfected with miR-493-5p mimic or inhibitor, and corresponding control, were inoculated into six-well plates at 600 cells per well and cultured until visible clones formed. The cells were subsequently washed with phosphate-buffered saline (PBS; Servicebio, Wuhan, China), fixed with paraformaldehyde (Biosharp), and stained with crystal violet (Coolaber).

## 2.8 Wound-healing assay

AMC-HN-8 and CAL-27 cells transfected with miR-493-5p mimic or inhibitor, and corresponding control, were cultured in six-well plates until they reached 90% confluence. A scratch wound was generated using a 1-mL pipette tip. Cells were then rinsed with PBS for nonadherent cell removal, and the remaining cells were cultured for 0 and 24 h in a serum-free medium. Finally, wound closures were measured at appropriate timepoints and analysed using Image J. % wound closed = (wound area at 0 h- wound area at 24 h)/wound area at 0 h × 100%.

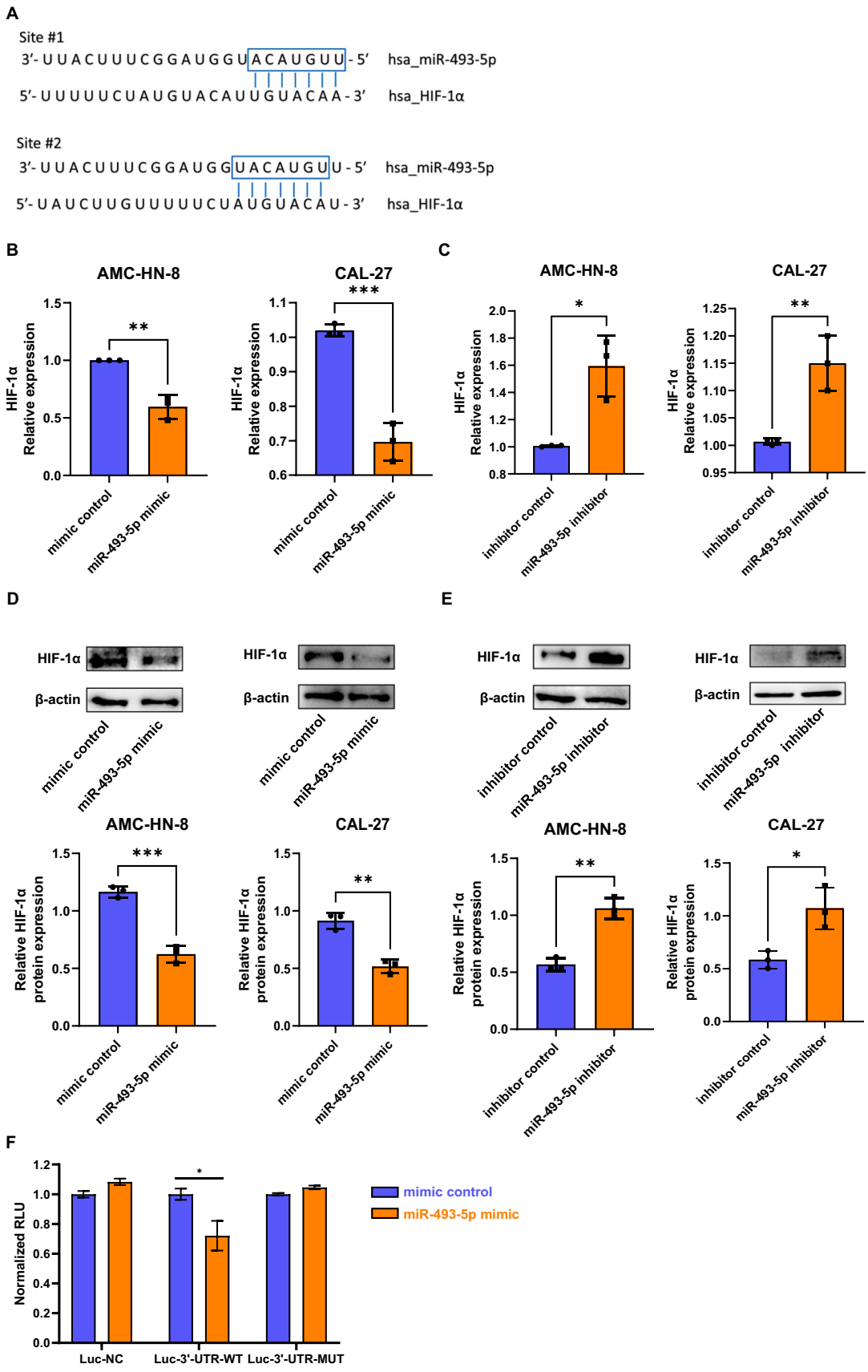
A
Site #1
3′- U U A C U U U C G G A U G G U A C A U G U U - 5′ hsa_miR-493-5p
5′- U U U U U C U A U G U A C A U U G U A C A A - 3′ hsa_HIF-1α
Site #2
3′- U U A C U U U C G G A U G G U A C A U G U U - 5′ hsa_miR-493-5p
5′- U A U C U U G U U U U U C U A U G U A C A U - 3′ hsa_HIF-1α
B
AMC-HN-8
CAL-27
HIF-1α Relative expression
mimic control
miR-493-5p mimic
C
AMC-HN-8
CAL-27
HIF-1α Relative expression
inhibitor control
miR-493-5p inhibitor
D
HIF-1α
β-actin
mimic control
miR-493-5p mimic
AMC-HN-8
CAL-27
Relative HIF-1α protein expression
E
HIF-1α
β-actin
inhibitor control
miR-493-5p inhibitor
AMC-HN-8
CAL-27
Relative HIF-1α protein expression
F
Normalized RLU
Luc-NC
Luc-3′-UTR-WT
Luc-3′-UTR-MUT
mimic control
miR-493-5p mimic

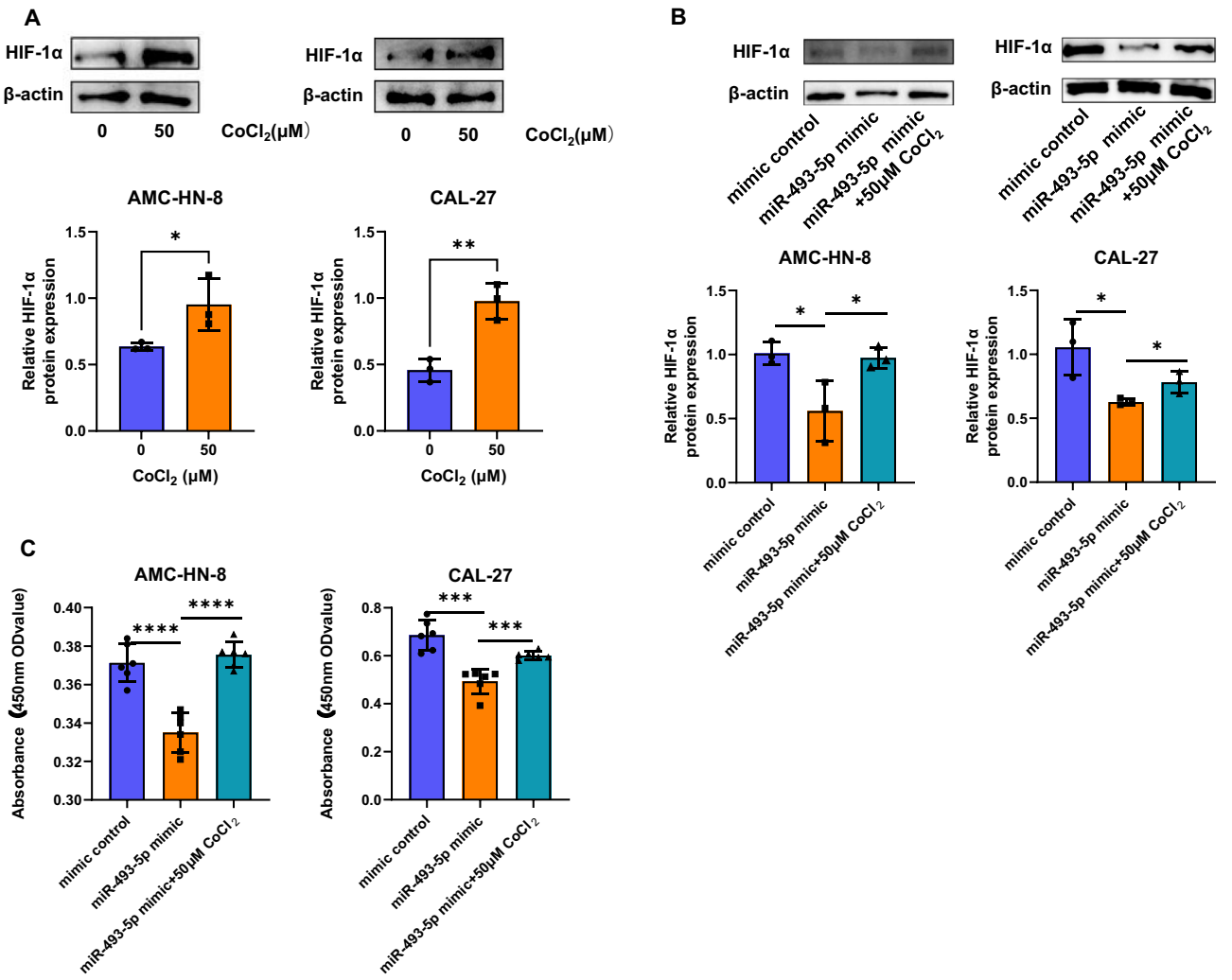


**Fig. 4** $CoCl_2$ induces HIF-1α expression in AMC-HN-8 and CAL-27 cells and reverses cell proliferation reduction. **A** HIF-1α overexpression in $CoCl_2$-treated AMC-HN-8 and CAL-27 cells. **B** HIF-1α expression rescued in miR-493-5p mimic-transfected AMC-HN-8 and CAL-27 cells. **C** $COCl_2$ treatment rescued cell proliferation in miR-493-5p mimic-transfected AMC-HN-8 and CAL-27 cells. *$p < 0.05$, **$p < 0.005$, ***$p < 0.0005$, ****$p < 0.0001$

## 2.9 Dual-luciferase reporter gene assay

The TargetScan database was used to identify a putative miR-493-5p binding site in wild-type (WT) 3′-UTR fragment of *HIF1 A* mRNA, after which luciferase reporter plasmids HIF-1α-WT and HIF-1α-mutant (MUT) were generated and separately cloned into psiCHECK2 vector (Sangon, Shanghai, China). The cells were then transfected with the reporter plasmid and miR-493-5p mimic or control using Lipofectamine 3000 (Thermo). After 48 h, cells were collected, and a Dual Luciferase Reporter Assay kit (Vazyme) was used for luciferase activity determination, according to the manufacturer's instructions.

## 2.10 Animal experiments

All animal experiments, consistent with laboratory animal welfare protocols, were approved by the Committee on Animal Ethics of Yantai Yuhuangding Hospital, and all procedures were conducted in accordance with to NIH Guidelines for the Care and Use of Laboratory Animals. In total, 5-week-old male C57BL6/J mice (n = 14; weight at the beginning of the study = 19.40 ± 0.51 g) were purchased from Beijing Vital River Laboratory Animal Technology (China) and divided into two

groups (n = 7 per group): LV-NC mimic and LV-miR-493-5p. All mice were maintained at 25 °C ± 2 °C in a clean atmosphere with 50% relative humidity under a 12-h dark–light cycle. The mice had ad libitum access to food and water. SCC VII cells stably transfected with LV-NC mimic or LV-miR-493-5p ($2 \times 10^6$ cells in 100 µL of PBS) were injected subcutaneously into the right underarm of each mouse [25]. Tumour width and length were assessed every 1 or 2 days, and tumour size was calculated as volume ($mm^3$) = [length (mm) × width $(mm)^2$]/2. Mice were sacrificed through cervical dislocation 15 days after cancer cell inoculation. The maximal tumour size/burden was not exceeded 2000 $mm^3$ in the present study, which was permitted by the Committee on Animal Ethics of Yantai Yuhuangding Hospital.

### 2.11 Statistics analysis

Statistical analyses were performed via SPSS (version 25.0, IBM Corp.) and GraphPad Prism (version 9). The clinical characteristics of the two groups in HNSCC were assessed by the $\chi 2$ test or Fisher's exact test. Paired tissue samples were subjected to Paired Samples *t*-test. Other data were subjected to Student's *t* test. All data are expressed as the mean ± standard deviation (mean ± SD), and $p < 0.05$ was considered to indicate statistical significance.

## 3 Results

### 3.1 MiR-493-5p expression is low and beneficial to prognosis in HNSCC

To investigate the role of miR-493-5p in HNSCC pathogenesis, we first determined the expression levels of miR-493-5p based on TCGA-HNSC dataset. miR-493-5p expression was significantly lower in HNSCC tissues than in normal tissues (Fig. 1A). We then verified the miR-493-5p expression status in our collected samples (n = 20) through qRT-PCR. These results also demonstrated that miR-493-5p expression was significantly lower in HNSCC tissue samples than in the matched paracancerous tissue samples (Fig. 1B). Subsequently, qRT-PCR results showed that the expression of miR-493-5p was lower in HNSCC cell lines than in normal epithelial cells (Fig. 1C). In addition, patients from the TCGA-HNSC data set were divided into low and high expression groups based on the median miR-493-5p expression level. Kaplan–Meier survival curves revealed that HNSCC patients with higher miR-493-5p expression had better prognosis (Fig. 1D). And the prognostic difference of HNSCC patients between the high and low miR-493-5p expression group was not influenced by age, gender, clinical stage and TNM stage (Table 2).

### 3.2 MiR-493-5p inhibits HNSCC cell proliferation and migration

Because miR-493-5p expression was significantly lower in HNSCC tissues than in the adjacent tissues, it may have a tumour-repressive role in HNSCC. To study the effects of miR-493-5p on HNSCC cell function, we transfected the laryngeal squamous cell carcinoma cell line AMC-HN-8 and tongue squamous cell carcinoma cell line CAL-27 with a miR-493-5p mimic or inhibitor. The expression of miR-493-5p in transfected AMC-HN-8 and CAL-27 cells was detected by qRT-PCR to verify the effect of miR-493-5p mimic and inhibitor (Fig. 2A, B). Subsequent cell experiments revealed that the miR-493-5p mimic reduced cell proliferation significantly, whereas the miR-493-5p inhibitor promoted it (Fig. 2C, D). These findings were corroborated by our colony formation assay results: the miR-493-5p mimic suppressed the colony-forming potential of the AMC-HN-8 and CAL-27 cells, but the miR-493-5p inhibitor did not (Fig. 2E, F). Moreover, the wound-healing assay revealed that the miR-493-5p mimic considerably restrained cell migratory properties, whereas the miR-493-5p inhibitor led to contradictory results (Fig. 2G, H).

### 3.3 MiR-493-5p represses HIF-1α expression by targeting HIF-1α

We used the TargetScan database to identify the binding sites between miR-493-5p and HIF-1α and found that miR-493-5p and the 3′-UTR of *HIF1 A* mRNA have two potential complementary regions (Fig. 3A). Subsequently, we noted that in AMC-HN-8 and CAL-27 cells, increased miR-493-5p expression led to *HIF1 A* mRNA downregulation, whereas repression of miR-493-5p expression resulted in its upregulation (Fig. 3B, C). Similarly, Western blotting revealed that the miR-493-5p mimic reduced HIF-1α expression, whereas the miR-493-5p inhibitor upregulated it (Fig. 3D,

**Fig. 5** MiR-493-5p suppresses HNSCC cell proliferation in vivo and in vitro. **A** MiR-493-5p overexpression in SCC VII cells. **B** Differences in ▶ SCC VII cell proliferation between the LV-miR-493-5p and LV-NC mimic groups measured using CCK-8 assay. **C** Differences in colony-forming potential of SCC VII cells between the LV-miR-493-5p and LV-NC mimic groups measured using colony formation assay. **D** HIF-1α expression in SCC VII cell between the LV-miR-493-5p and LV-NC mimic groups. **E** Schematic representation of our animal experiments. Mice were divided into LV-NC mimic and LV-miR-493-5p groups. Tumour volume was estimated using a vernier calliper over postinjection days 6–15. Representative images of tumours isolated from C57BL6/J mice are presented. **F** Tumour growth curves of LV-miR-493-5p and LV-NC mimic group. **G** Scatter plot of tumour volume at the time the mice were sacrificed on day 15 in the LV-miR-493-5p and LV-NC mimic groups. **H** Scatter plot of tumour weight at the time the mice were sacrificed on day 15 in the LV-miR-493-5p and LV-NC mimic group. **I** C57BL6/J mice body weight curve of the LV-miR-493-5p and LV-NC mimic groups. *$p < 0.05$, **$p < 0.005$, ***$p < 0.0005$, ****$p < 0.0001$

E). Moreover, the dual-luciferase reporter gene assay results demonstrated that induced miR-493-5p expression significantly reduced the luciferase activity of cells with HIF-1α-WT; however, this effect was not significant in cells with HIF-1α-MUT (Fig. 3F). Thus, miR-493-5p may target and downregulate HIF-1α expression.

### 3.4 MiR-493-5p regulates HNSCC cell proliferation by targeting HIF-1α

We initially assessed the HIF-1α-targeting effects of miR-493-5p by incubating AMC-HN-8 and CAL-27 cells with $CoCl_2$, a HIF-1α inducer, for 24 h. $CoCl_2$ was noted to induce significant HIF-1α expression (Fig. 4A). Next, miR-493-5p mimic-transfected cells were treated with $CoCl_2$ similarly. The results indicated that $CoCl_2$ rescued miR-493-5p-downregulated expression of HIF-1α (Fig. 4B). Subsequent cell experiments further illustrated that $CoCl_2$ addition rescued the miR-493-5p mimic-induced decrease in cell proliferation, which may be related to increased HIF-1α expression (Fig. 4C).

### 3.5 MiR-493-5p suppresses HNSCC progression in vitro and in vivo

Our qRT-PCR results demonstrated that LV-miR-493-5p led to effective construction of miR-493-5p-overexpressing stable SCC VII cells (Fig. 5A). Cell proliferation and colony formation assays revealed that LV-miR-493-5p considerably reduced cell proliferation in vitro (Fig. 5B, C). Western blotting revealed that the LV-miR-493-5p reduced HIF-1α expression in SCC VII cells (Fig. 5D). Then, we evaluated the suppressive activity of miR-493-5p in vivo by using mice models constructed using treated SCC VII cell lines (Fig. 5E). The results demonstrated that LV-miR-493-5p significantly reduced tumour volume and weight in vivo (Fig. 5F–H). However, it did not affect the body weight of the mice significantly (Fig. 5I).

### 3.6 MiR-493-5p may associate with glycolysis in HNSCC

To explore the association among miR-493-5p, HIF-1α and HNSCC further, we used Western blotting for glycolysis proteins. In both AMC-HN-8 and CAL-27 cells, miR-493-5p mimic transfection was associated with significant reductions in GLUT1, LDHK and PDHK1 levels (Fig. 6A), whereas miR-493-5p inhibitor transfection was the opposite (Fig. 6B). Thus, these results suggested that miR-493-5p may regulate HIF-1α, thereby involving in glycolysis activity in HNSCC cells.

### 3.7 MiR-493-5p may associate with EMT in HNSCC

E-cadherin expression upregulated and N-cadherin expression downregulated in miR-493-5p mimic-transfected AMC-HN-8 and CAL-27 cells (Fig. 7A), which was opposite in cells transfected with miR-493-5p inhibitor (Fig. 7B).This result suggested the presence of another mechanism where miR-493-5p may associate with EMT in HNSCC cells.

## 4 Discussion

Although many recent studies have focused on HNSCC pathogenesis and treatment, the prognosis of the affected patients has not improved significantly [26]. Therefore, clarifying the mechanisms underlying HNSCC is essential for improving patient prognosis and prolonging survival. Studies have shown that miRNAs, such as miR-96-5p [27],

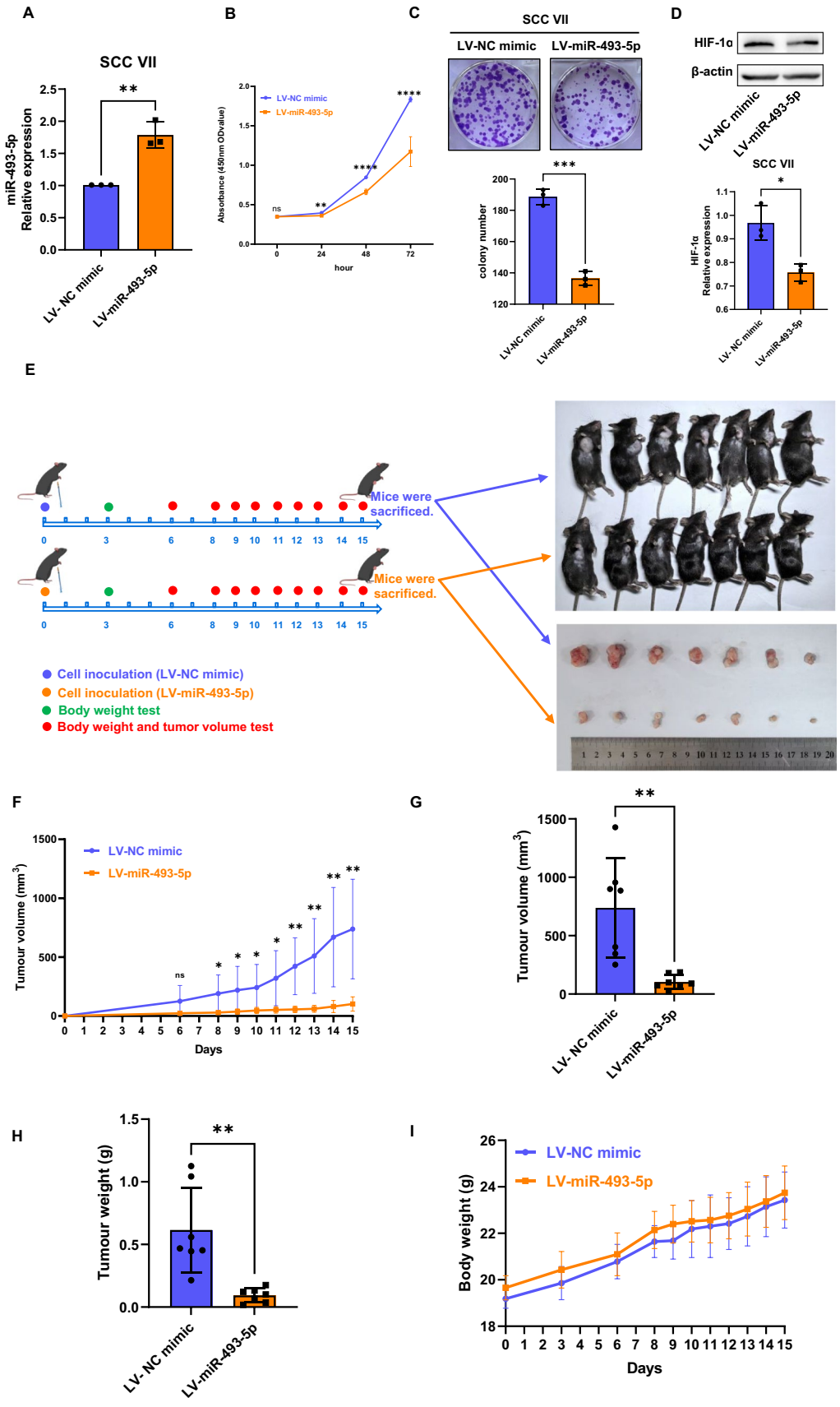
A
SCC VII
miR-493-5p Relative expression
LV- NC mimic
LV-miR-493-5p
B
LV-NC mimic
LV-miR-493-5p
Absorbance (450nm ODvalue)
hour
C
SCC VII
LV-NC mimic
LV-miR-493-5p
colony number
D
HIF-1α
β-actin
SCC VII
HIF-1α Relative expression
E
Mice were sacrificed.
Mice were sacrificed.
Cell inoculation (LV-NC mimic)
Cell inoculation (LV-miR-493-5p)
Body weight test
Body weight and tumor volume test
F
LV-NC mimic
LV-miR-493-5p
Tumour volume (mm3)
Days
G
Tumour volume (mm3)
LV- NC mimic
LV-miR-493-5p
H
Tumour weight (g)
LV- NC mimic
LV-miR-493-5p
I
LV-NC mimic
LV-miR-493-5p
Body weight (g)
Days

**Fig. 6** MiR-493-5p affects glycolysis-associated protein expression. **A** GLUT1, LDHK and PDHK1 expression downregulated in miR-493-5p mimic-transfected AMC-HN-8 and CAL-27 cells. **B** GLUT1, LDHK and PDHK1 expression upregulated in miR-493-5p inhibitor-transfected AMC-HN-8 and CAL-27 cells. $^{*}p < 0.05$, $^{**}p < 0.005$

miR-30a/e-3p [28], miR-34a [29], miR-411-5p [30], and miR-34a-5p [31], can regulate HNSCC progression. However, the impact of miR-493-5p on HNSCC has not been explored thus far. Here, we detected miR-493-5p downregulation in HNSCC tissues. Mechanistically, this miRNA, which can suppress HNSCC cell migration and proliferation by targeting HIF-1α, may be related to glycolysis and EMT. Taken together, these results highlight the miR-493-5p/HIF-1α axis as a viable therapeutic target for HNSCC.

Hypoxia commonly occurs during tumour development and progression and promotes HIF activation [32]. HIF-1α, the most important HIF, activates hypoxia-related transcriptional responses [33]. Identifying miRNA target genes is vital to understanding how they affect oncogenic processes. Subsequent analyses revealed the ability of miR-493-5p to bind to the 3′-UTR of *HIF1 A* mRNA, suggesting a potential mechanism whereby this miRNA may influence oncogenic processes. After transfection into two HNSCC cell lines, the miR-493-5p mimic led to HIF-1α knockdown at both the mRNA and protein levels. Moreover, miR-493-5p regulated a luciferase reporter harbouring a WT, but not a mutant version, of the *HIF1 A* mRNA 3′-UTR, consistent with the ability of this miRNA to suppress HIF-1α expression directly. To our knowledge, this is the first study to demonstrate the ability of miR-493-5p to suppress HNSCC oncogenesis via targeting HIF-1α.

Abnormal glucose metabolism is one of the major metabolic changes occurring in cancer cells compared with normal cells; most cancer cells exhibit significantly increased glucose uptake and glycolysis rate to meet their need for rapid proliferation and metastasis [34]. HIF-1α promotes glycolytic metabolism in tumour cells, which can promote the shift to glycolysis through PDHK1 upregulation, leading to PDHK1-dependent glucose metabolism reprogramming [19–21]. In the current study, we found that the expression of some glycolysis proteins including PDHK1, LDHA, and GLUT-1, was decreased in HNSCC cells transfected with miR-493-5p mimic, while their expression was increased in cells transfected with miR-493-5p inhibitor. Therefore, miR-493-5p may be involved in the glycolysis in HNSCC.

Hypoxia can also induce EMT—a cellular programme crucial for embryogenesis, wound healing, and malignant progression. EMT confers cancer cells with the potential to increase tumorigenesis and metastasis [35, 36]. Promotion of HIF-1α expression leads to a hypoxic tumour microenvironment, which then induces EMT and thus enhances tumour invasion and migration ability [22]. In the current study, we found that miR-493-5p expression was correlated with the expression of EMT-related proteins including E-cadherin and N-cadherin. Therefore, miR-493-5p may also be related to EMT in HNSCC.

However, our study has some limitations. Firstly, we only focused on immediate or short-term outcomes to investigate the inhibitory effects of miR-493-5p on HNSCC in vivo and in vitro. Secondly, although widely used for HNSCC in vivo studies, the origin of SCC VII cells is somewhat controversial and may not originate from the oral cavity. Finally, we did not further explore the specific mechanism by which miR-493-5p/HIF-1α regulates EMT and glycolytic processes. Therefore, we plan to design experiments to verify the long-term effect and therapeutic effects of targeting miR-493-5p on HNSCC, perform more extensive in vivo, as well as to further explore the processes of hypoxia, EMT, and glycolysis. In the future, we will focus on translational research of miR-493-5p for clinical application, and we believe that miR-493-5p may become a viable target for HNSCC diagnosis and treatment.

## 5 Conclusions

In summary, our results highlighted miR-493-5p as a novel mediator of anticancer activity in HNSCC, which can suppress HIF-1α by targeting it, to impair cell proliferation and migration, and may be associated with glycolysis and EMT. The miR-493-5p/HIF-1α/glycolysis or miR-493-5p/HIF-1α/EMT axis may thus represent a potential target for HNSCC treatment.

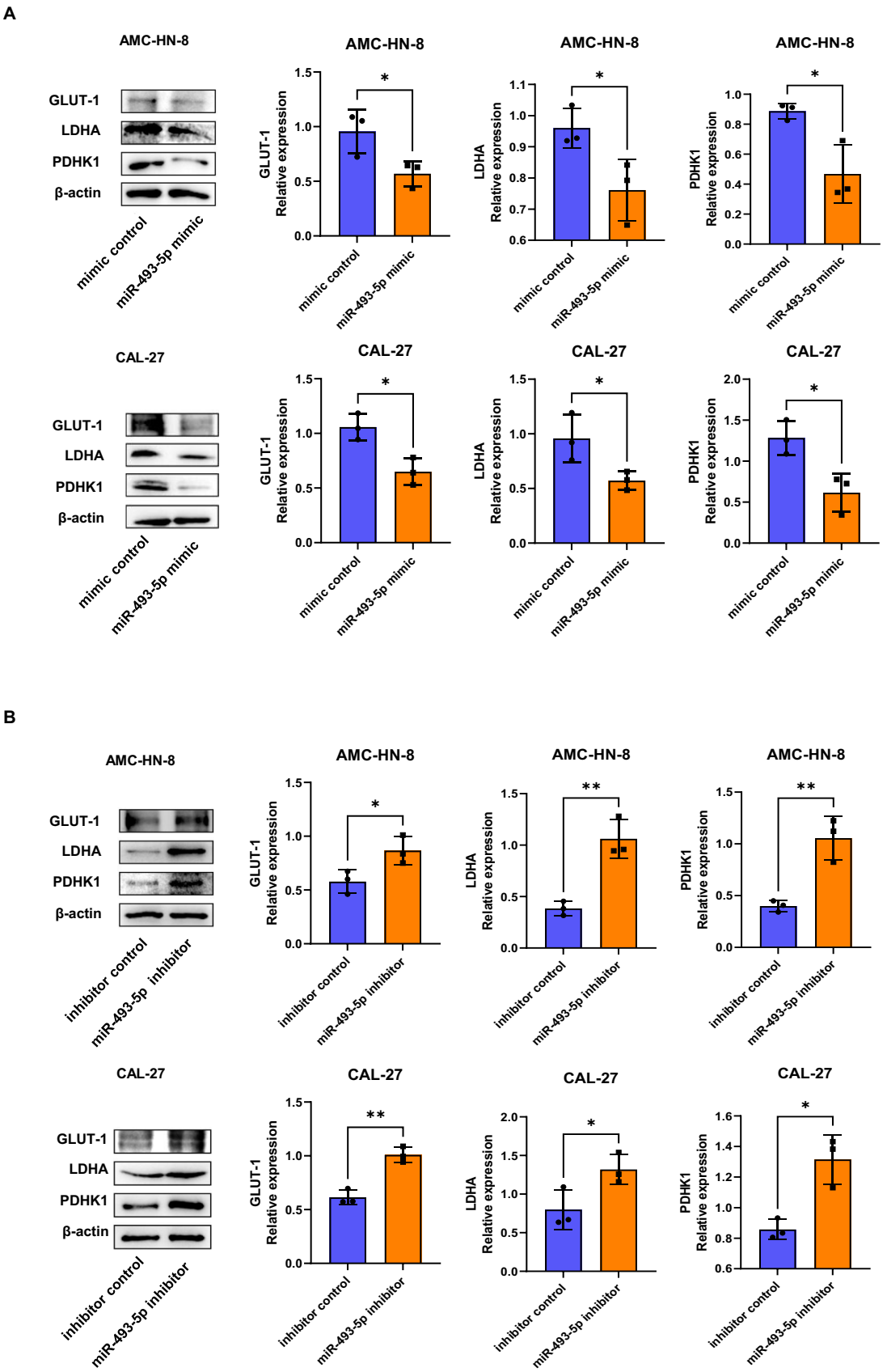
A
AMC-HN-8
GLUT-1
LDHA
PDHK1
β-actin
mimic control
miR-493-5p mimic
GLUT-1 Relative expression
LDHA Relative expression
PDHK1 Relative expression
CAL-27
B
inhibitor control
miR-493-5p inhibitor

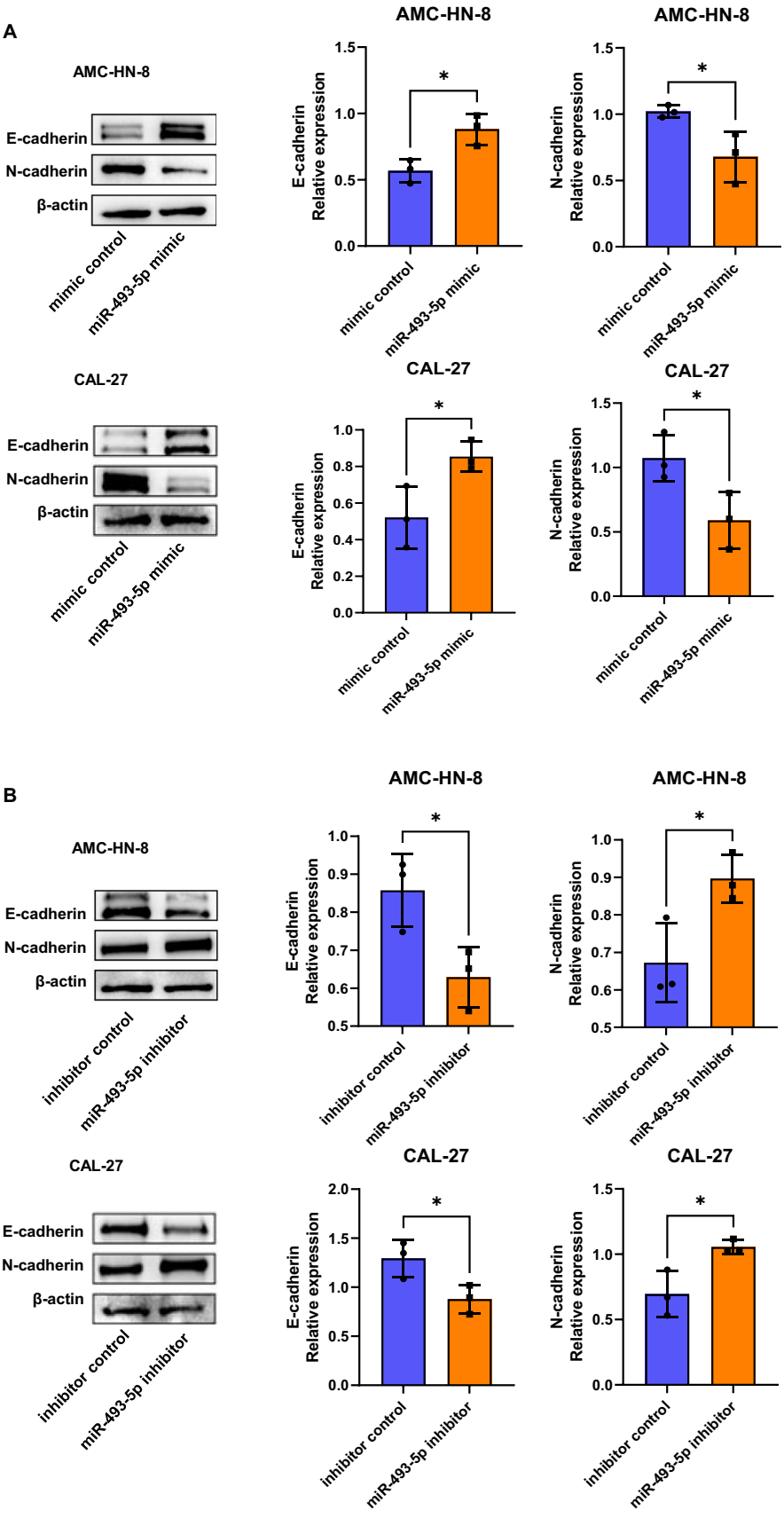


**Fig. 7** MiR-493-5p affects EMT-associated protein expression. **A** E-cadherin expression upregulated and N-cadherin expression downregulated in miR-493-5p mimic-transfected AMC-HN-8 and CAL-27 cells. **B** E-cadherin expression downregulated and N-cadherin expression upregulated in miR-493-5p inhibitor-transfected AMC-HN-8 and CAL-27 cells. *$p < 0.05$

**Acknowledgements** This work was supported by the Taishan Scholar Project (No.ts20190991), the Key R&D Project of Shandong Province (2022 CXPT023), Shandong Medical Association Clinical Research Fund-Qilu special fund YXH2022ZX02185, and Scholar Project of Yantai's "Double Hundreds plan".

**Author contributions** Jiahui Liu: Data curation, investigation, methodology, validation, visualization, writing–original draft, writing–review and editing. Ruxian Tian: Investigation, methodology and validation. Xi Chen: Investigation, methodology and validation. Qing Song: Methodology and investigation. Caiyu Sun: Methodology. Dongxian Li: Methodology. Yuhui Fang: Methodology. Shijun Lv: Methodology. Yumei Li: Conceptualization, formal analysis, funding acquisition, project administration, resources, supervision, writing–review and editing. Xicheng Song: Conceptualization, formal analysis, funding acquisition, project administration, resources, supervision, writing–review and editing.

**Funding** This work was supported by the Taishan Scholar Project (No.ts20190991), the Key R&D Project of Shandong Province (2022 CXPT023), Shandong Medical Association Clinical Research Fund-Qilu special fund YXH2022ZX02185, and Scholar Project of Yantai's "Double Hundreds plan".

**Data availability** Data is provided within the manuscript. All relevant data supporting this study's findings are available from the corresponding author upon request.

**Code availability** Not applicable.

## Declarations

**Competing interests** The authors declare no competing interests.



## References

1. Bray F, Laversanne M, Sung H, Ferlay J, Siegel RL, Soerjomataram I, et al. Global cancer statistics 2022: GLOBOCAN estimates of incidence and mortality worldwide for 36 cancers in 185 countries. CA Cancer J Clin. 2024;74(3):229–63. https://doi.org/10.3322/caac.21834.
2. Johnson DE, Burtness B, Leemans CR, Lui VWY, Bauman JE, Grandis JR. Head and neck squamous cell carcinoma. Nat Rev Dis Primers. 2020;6:92. https://doi.org/10.1038/s41572-020-00224-3.
3. Gormley M, Creaney G, Schache A, Ingarfield K, Conway DI. Reviewing the epidemiology of head and neck cancer: definitions, trends and risk factors. Br Dent J. 2022;233(9):780–6. https://doi.org/10.1038/s41415-022-5166-x.
4. Mattick JS. Non-coding RNAs: the architects of eukaryotic complexity. EMBO Rep. 2001;2:986–91. https://doi.org/10.1093/embo-reports/kve230.
5. Huang Y. The novel regulatory role of lncRNA-miRNA-mRNA axis in cardiovascular diseases. J Cell Mol Med. 2018;22:5768–75. https://doi.org/10.1111/jcmm.13866.
6. Calin GA, Dumitru CD, Shimizu M, Bichi R, Zupo S, Noch E, et al. Frequent deletions and down-regulation of micro- RNA genes miR15 and miR16 at 13q14 in chronic lymphocytic leukemia. Proc Natl Acad Sci USA. 2002;99:15524–9. https://doi.org/10.1073/pnas.242606799.
7. Cui FC, Chen Y, Wu XY, Hu M, Qin WS. MicroRNA-493–5p suppresses colorectal cancer progression via the PI3K-Akt-FoxO3a signaling pathway. Eur Rev Med Pharmacol Sci. 2020;24:4212–23. https://doi.org/10.26355/eurrev_202004_21001.
8. Liu H, Li Z, Sun H. MiR-493-5p inhibits the malignant development of gliomas via suppressing E2F3-mediated dysfunctions of P53 and PI3K/AKT pathways. Clin Transl Oncol. 2022;24:363–70. https://doi.org/10.1007/s12094-021-02698-3.
9. Feng N, Guo Z, Wu X, Tian Y, Li Y, Geng Y, et al. Circ_PIP5K1A regulates cisplatin resistance and malignant progression in non-small cell lung cancer cells and xenograft murine model via depending on miR-493-5p/ROCK1 axis. Respir Res. 2021;22:248. https://doi.org/10.1186/s12931-021-01840-7.
10. Zhao J, Xu T, Wang F, Cai W, Chen L. miR-493-5p suppresses hepatocellular carcinoma cell proliferation through targeting GP73. Biomed Pharmacother. 2017;90:744–51. https://doi.org/10.1016/j.biopha.2017.04.029.
11. Wang X, Wu T, Wang P, Yang L, Li Q, Wang J, et al. Circular RNA 103862 promotes proliferation and invasion of laryngeal squamous cell carcinoma cells through the miR-493-5p/GOLM1 axis. Front Oncol. 2020;10:1064. https://doi.org/10.3389/fonc.2020.01064.
12. Zhao L, Feng X, Song X, Zhou H, Zhao Y, Cheng L, et al. miR-493-5p attenuates the invasiveness and tumorigenicity in human breast cancer by targeting FUT4. Oncol Rep. 2016;36:1007–15. https://doi.org/10.3892/or.2016.4882.
13. Liu Q, Luo J, Wang H, Zhang L, Jin G. SNHG1 functions as an oncogenic lncRNA and promotes osteosarcoma progression by up-regulating S100A6 via miR-493-5p. Acta Biochim Biophys Sin. 2022;54:137–47. https://doi.org/10.3724/abbs.2021014.

14. LaGory EL, Giaccia AJ. The ever-expanding role of HIF in tumour and stromal biology. Nat Cell Biol. 2016;18:356–65. https://doi.org/10.1038/ncb3330.
15. Cao L, Wang M, Dong Y, Xu B, Chen J, Ding Y, et al. Circular RNA circRNF20 promotes breast cancer tumorigenesis and Warburg effect through miR-487a/HIF-1α/HK2. Cell Death Dis. 2020;11:145. https://doi.org/10.1038/s41419-020-2336-0.
16. Hu K, Ding Y, Zhu H, Jing X, He W, Yu H, et al. Glutamate dehydrogenase1 supports HIF-1α stability to promote colorectal tumorigenesis under hypoxia. EMBO J. 2023;42:e112675. https://doi.org/10.15252/embj.2022112675.
17. Chen Y, Liu L, Xia L, Wu N, Wang Y, Li H, et al. TRPM7 silencing modulates glucose metabolic reprogramming to inhibit the growth of ovarian cancer by enhancing AMPK activation to promote HIF-1α degradation. J Exp Clin Cancer Res. 2022;41:44. https://doi.org/10.1186/s13046-022-02252-1.
18. Wang M, Chen H, He X, Zhao X, Zhang H, Wang Y, et al. Artemisinin inhibits the development of esophageal cancer by targeting HIF-1α to reduce glycolysis levels. J Gastrointest Oncol. 2022;13:2144–53. https://doi.org/10.21037/jgo-22-877.
19. Kim JW, Tchernyshyov I, Semenza GL, Dang CV. HIF-1-mediated expression of pyruvate dehydrogenase kinase: a metabolic switch required for cellular adaptation to hypoxia. Cell Metab. 2006;3:177–85. https://doi.org/10.1016/j.cmet.2006.02.002.
20. Papandreou I, Cairns RA, Fontana L, Lim AL, Denko NC. HIF-1 mediates adaptation to hypoxia by actively downregulating mitochondrial oxygen consumption. Cell Metab. 2006;3:187–97. https://doi.org/10.1016/j.cmet.2006.01.012.
21. Lu CW, Lin SC, Chen KF, Lai YY, Tsai SJ. Induction of pyruvate dehydrogenase kinase-3 by hypoxia-inducible factor-1 promotes metabolic switch and drug resistance. J Biol Chem. 2008;283:28106–14. https://doi.org/10.1074/jbc.M803508200.
22. Du J, Sun B, Zhao X, Gu Q, Dong X, Mo J, et al. Hypoxia promotes vasculogenic mimicry formation by inducing epithelial-mesenchymal transition in ovarian carcinoma. Gynecol Oncol. 2014;133:575–83. https://doi.org/10.1016/j.ygyno.2014.02.034.
23. McGeary SE, Lin KS, Shi CY, Pham TM, Bisaria N, Kelley GM, et al. The biochemical basis of microRNA targeting efficacy. Science. 2019;366:6472. https://doi.org/10.1126/science.aav1741.
24. Duan Y, Zhou M, Ye B, Yue K, Qiao F, Wang Y, et al. Hypoxia-induced miR-5100 promotes exosome-mediated activation of cancer-associated fibroblasts and metastasis of head and neck squamous cell carcinoma. Cell Death Dis. 2024;15(3):215. https://doi.org/10.1038/s41419-024-06587-9.
25. O'Malley BW Jr, Cope KA, Johnson CS, Schwartz MR. A new immunocompetent murine model for oral cancer. Arch Otolaryngol. 1997;123(1):20–4. https://doi.org/10.1001/archotol.1997.01900010022003.
26. Budach V, Tinhofer I. Novel prognostic clinical factors and biomarkers for outcome prediction in head and neck cancer: a systematic review. Lancet Oncol. 2019;20:e313–26. https://doi.org/10.1016/s1470-2045(19)30177-9.
27. Vahabi M, Pulito C, Sacconi A, Donzelli S, D'Andrea M, Manciocco V, et al. miR-96-5p targets PTEN expression affecting radio-chemosensitivity of HNSCC cells. J Exp Clin Cancer Res. 2019;38:141. https://doi.org/10.1186/s13046-019-1119-x.
28. Conrad O, Burgy M, Foppolo S, Jehl A, Thiéry A, Guihard S, et al. Tumor-suppressive and immunomodulating activity of miR-30a-3p and miR-30e-3p in HNSCC cells and tumoroids. Int J Mol Sci. 2023. https://doi.org/10.3390/ijms241311178.
29. Zhang J, Wang Y, Chen X, Zhou Y, Jiang F, Chen J, et al. MiR-34a suppresses amphiregulin and tumor metastatic potential of head and neck squamous cell carcinoma (HNSCC). Oncotarget. 2015;6:7454–69. https://doi.org/10.18632/oncotarget.3148.
30. Zhang C, Wang H, Deng M, He L, Ping F, He Y, et al. Upregulated miR-411-5p levels promote lymph node metastasis by targeting RYBP in head and neck squamous cell carcinoma. Int J Mol Med. 2021. https://doi.org/10.3892/ijmm.2021.4869.
31. Li X, Zhao S, Fu Y, Zhang P, Zhang Z, Cheng J, et al. miR-34a-5p functions as a tumor suppressor in head and neck squamous cell cancer progression by targeting Flotillin-2. Int J Biol Sci. 2021;17:4327–39. https://doi.org/10.7150/ijbs.64851.
32. Yasuda H. Solid tumor physiology and hypoxia-induced chemo/radio-resistance: novel strategy for cancer therapy: nitric oxide donor as a therapeutic enhancer. Nitric Oxide Biol Chem. 2008;19:205–16. https://doi.org/10.1016/j.niox.2008.04.026.
33. Semenza GL. HIF-1 and human disease: one highly involved factor. Genes Dev. 2000;14:1983–91.
34. Lu J, Tan M, Cai Q. The Warburg effect in tumor progression: mitochondrial oxidative metabolism as an anti-metastasis mechanism. Cancer Lett. 2015;356:156–64. https://doi.org/10.1016/j.canlet.2014.04.001.
35. Dongre A, Weinberg RA. New insights into the mechanisms of epithelial-mesenchymal transition and implications for cancer. Nat Rev Mol Cell Biol. 2019;20:69–84. https://doi.org/10.1038/s41580-018-0080-4.
36. Liu K, Sun B, Zhao X, Wang X, Li Y, Qiu Z, et al. Hypoxia induced epithelial-mesenchymal transition and vasculogenic mimicry formation by promoting Bcl-2/Twist1 cooperation. Exp Mol Pathol. 2015;99:383–91. https://doi.org/10.1016/j.yexmp.2015.08.009.